SELF-REFLECTIVE REINFORCEMENT LEARNING FOR DIFFUSION-BASED IMAGE REASONING GENERATION

Anonymous authorsPaper under double-blind review

ABSTRACT

Recent years have witnessed the wonderful effects of diffusion models in generative task. However, existing image generation methods still suffer from the significant "reasoning-oriented generative" dilemma. Motivated by the success of Chain of Thought (CoT) and Reinforcement Learning (RL) in LLMs, we propose SRRL, a self-reflective RL algorithm for diffusion models to achieve reasoning generation of logical images by performing reflection and iteration across generation trajectories. The intermediate samples in the denoising process carry noise, making accurate reward evaluation difficult. To address this challenge, SRRL treats the entire denoising trajectory as a CoT step with multi-round reflective denoising process and introduces condition guided forward process, which allows for reflective iteration between CoT steps. Through SRRL-based iterative diffusion training, we introduce image reasoning through CoT into generation tasks adhering to physical laws and unconventional physical phenomena for the first time. Notably, experimental results of case study exhibit that the superior performance of our SRRL algorithm even compared with advanced T2I models.

1 Introduction

Recent years have witnessed the remarkable success of text-to-image (T2I) models (Ho et al., 2020; Ramesh et al., 2021; 2022). As the pioneering model among many T2I models, diffusion models have demonstrated powerful abilities in generating realistic images (Saharia et al., 2022; Ramesh et al., 2022; Podell et al., 2023; Ma et al.; Zhang et al., 2023; Ruiz et al., 2023; Ma et al., 2024). Existing works introduce ControlNet (Zhang et al., 2023) and T2I-Adapter (Mou et al., 2024) to enhance the controllability of image generation. However, these models still lack the ability of reflective reasoning, resulting in issues that images do not adhere to physical laws, where images may be visually stunning but logically inconsistent (Jiang et al., 2024; Huang et al., 2023).

Reinforcement learning (RL) based training methods (Black et al., 2023; Wallace et al., 2024; Fan et al., 2023; Hu et al., 2025; Majumder et al., 2024), including Direct Preference Optimization (DPO) and Proximal Policy Optimization (PPO), have recently been integrated into diffusion models to enhance specific capabilities, such as text-image alignment and human feedback alignment. DPO aligns diffusion models to human preferences by directly optimizing on comparison data, relying on high-quality user feedback, which leads to high collection costs. PPO optimizes the parameters by considering the step-by-step denoising process as a multi-step decision-making process (Black et al., 2023), which treats noisy samples at each timestep as states, denoising process at each timestep as actions, and evaluated score of the final images as rewards. However, PPO optimizes the entire trajectory according to the final images by outcome reward models (ORMs), lacking the ability for reflective reasoning, which results in insufficient capabilities of complex logical image generation.

Reflective reasoning through Chain-of-thought (CoT) (Wei et al., 2022) has been widely explored in LLMs by allowing models to decompose complex problems into several intermediate reasoning steps (Guo et al., 2025a; Jaech et al., 2024; Hui et al., 2024; Lightman et al., 2023). Despite CoT being widely used in LLMs to increase the ability of solving complex NLP problems, there is relatively less work (Guo et al., 2025b; Jiang et al., 2025a) on enhancing reasoning capabilities in the field of image generation. Very recently, some works (Guo et al., 2025b; Jiang et al., 2025a) explore CoT in auto-regressive image generation architecture. However, there remains a significant challenge, which is exploring introducing CoT into diffusion models to enhance image reasoning capabilities. The

056

058

060

061

066

067

068

069

071

072

073

074

075

076

077

079

081

082

083

084

087

090

091

092

093 094

095

096

098

099

100

101

102

103

104

105

106

107

Figure 1: Illustration of self-reflective reasoning step. Through self-reflective processes of repeated denoising and re-noising, diffusion models achieve image reasoning generation adhered to physical laws and counterintuitive physical phenomena.

step-by-step diffusion denoising process produces noisy intermediate samples that are difficult to evaluate, thereby hindering the implementation of CoT reasoning during the denoising process.

In this paper, we present a novel self-reflective RL algorithm **SRRL** of diffusion models, introducing CoT into diffusion models to provide self-reflective capabilities by RL training to achieve image reasoning generation. Specifically, SRRL incorporates multi-round reflective denoising process and condition guided forward process, treating the entire diffusion denoising trajectory as a step and constructing CoT between different trajectories instead of in a single denoising trajectory, which avoids the challenges of predicting rewards of noisy samples. Illustration of self-reflective reasoning step is shown in Fig. 1. With self-reflective capabilities, SRRL achieves image reasoning generation—for instance, ensuring that generated images adhere to physical laws, such as depicting plants growing taller with sunlight compared to those without in Fig. 3. Experimental results demonstrate that diffusion models trained by SRRL can generate images adhering to physical laws and counterintuitive scenarios. More impressively, images adhering to physical laws and counterintuitive physical phenomena generated through self-reflective reasoning of SRRL rival or surpass those generated by advanced T2I models recently.

Our contributions can be summarized as:

- We introduce a self-reflective RL algorithm SRRL, enabling diffusion models with the ability for self-reflective thinking and imagination.
- We explore introducing CoT into the generation process of diffusion models, allowing process reward models (PRMs) to address the issue of diffusion models being unable to self-reflect based on noisy intermediate results.
- Experimental results indicate that SRRL achieves image reasoning generation adhering to both physical laws and counterintuitive physical phenomena. Specifically, experimental samples of SRRL exhibit superior quality even compared to advanced T2I models recently.

2 RELATED WORK

2.1 Text-to-image Diffusion Models

Diffusion models are widely used in text-to-image (T2I) tasks due to their exceptional performance in generating high-quality images (Song et al., 2020b; Dhariwal & Nichol, 2021; Nichol & Dhariwal, 2021; Song & Ermon, 2020). Diffusion models generate images by denoising noisy images under the guidance of the text conditions. Many works, such as Stable Diffusion (Rombach et al., 2022), Imagen (Saharia et al., 2022), DALL-E (Ramesh et al., 2021), GPT-40 (Hurst et al., 2024), demonstrate the ability of diffusion models in T2I tasks. The alignment between text and images has become an important metric for improving the effectiveness of the model. Classifier-free guidance (CFG) (Ho & Salimans, 2022) is introduced into diffusion models to enhance text conditions and text-image alignment. Some works (Chung et al., 2024; Bradley & Nakkiran, 2024; Li et al., 2024) improve the generation quality and text-image alignment by optimizing CFG. Zigzag diffusion sampling (Bai et al., 2024) incorporates a self-reflection mechanism leveraging CFG to accumulate semantic information during inference process. However, they do not consider allowing models to learn reasoning, which leads to their inability to generate logical images adhering to physical laws.

2.2 REINFORCEMENT LEARNING OF DIFFUSION MODELS

Reinforcement Learning from Human Feedback (RLHF) (Ouyang et al., 2022) is employed for better alignment of diffusion models to human preferences. Some reward models (Hessel et al., 2021; Xu et al., 2023; Lin et al., 2024) are trained to enhance aesthetic quality, text-image alignment, and so on, to align with human preferences. Diffusion denoising process can be seen as a sequential decision-making problem (Black et al., 2023), allowing the application of RL algorithms (Black et al., 2023; Fan et al., 2023; Hu et al., 2025; Ren et al., 2024). DDPO (Black et al., 2023) is a policy gradient algorithm treating diffusion denoising process as Markov decision process and using proximal policy optimization (PPO) (Schulman et al., 2017) updates. However, these algorithms use outcome reward models (ORMs) due to the challenge of evaluating intermediate noisy images and cannot self-reflective reasoning based on a single denoising process.

2.3 Reflective Reasoning Through Chain-of-Thought

Large language models (LLMs) and multi-modal large language models (MLLMs) are discovered to simulate human thought process by reflective reasoning based on their understanding and generation skills (Meng et al., 2025; Yang et al., 2025; Jiang et al., 2025b). Recent works (Jaech et al., 2024; Guo et al., 2025a; Wei et al., 2022) incorporate Chain-of-Thought (CoT) to achieve superior performance in text generation tasks, such as mathematics (Zhang et al., 2024; Lu et al., 2023), coding (Jain et al., 2024), and image understanding (Huang et al., 2025) problems. On the contrary, the exploration of CoT in image generation has been more limited. Some works (Guo et al., 2025b; Jiang et al., 2025a) explore incorporating CoT in image generation tasks. However, it uses the auto-regressive architecture as the backbone, without exploring the potential of CoT in T2I diffusion models, which are more widely used in commercial applications.

3 METHOD

 In this section, we first introduce the training of diffusion models using reinforcement learning (RL) algorithms and self-reflective RL algorithm of diffusion models SRRL in Sec. 3.1. Then we propose multi-round reflective denoising process in Sec. 3.2 and condition guided forward process in Sec. 3.3. These two processes together constitute SRRL algorithm, which is illustrated in Fig. 2.

3.1 PROBLEM FORMULATION

3.1.1 REINFORCEMENT LEARNING TRAINING OF DIFFUSION MODELS

Text-to-image diffusion models generate images by progressively denoising noisy images. We follow the formulation of diffusion models in denoising diffusion probabilistic models (DDPMs) (Ho et al., 2020). Diffusion models are composed of two processes: forward process and denoising process.

Forward Process. Given a dataset with samples $x_0 \sim q_0(x_0|c)$ where q_0 is the data distribution and corresponding to text condition c, forward process is a Markov chain that gradually adds Gaussian noise into x_0 in T timesteps according to the variance schedule β_t :

$$q(x_t|x_{t-1}) = \mathcal{N}(x_t; \sqrt{1 - \beta_t} x_{t-1}, \beta_t \mathbf{I}), \qquad q(x_{1:T}|x_0) = \prod_{t=1}^T q(x_t|x_{t-1})$$
 (1)

Forward process constructs an approximate posterior distribution, and the goal of denoising process is to approximate it.

Denoising Process is a Markov chain, which can be seen as a Markov decision process (MDP).

$$p_{\theta}(x_{t-1}|x_t,c) = \mathcal{N}(x_{t-1}; \boldsymbol{\mu}_{\theta}(x_t,c,t), \boldsymbol{\Sigma}_t), \qquad p_{\theta}(x_{0:T}|c) = p(x_T) \prod_{t=1}^{T} p_{\theta}(x_{t-1}|x_t,c)$$
 (2)

where $\mu_{\theta}(x_t, c, t)$ is predicted by a diffusion model θ , and Σ_t is variance related to timestep t. Given samples x_0 and text condition $c \sim p(c)$, text-to-image diffusion models generate images according to text condition c. Classifier-free guidance (CFG) (Ho & Salimans, 2022) enhances text conditions to improve image generation quality by subtracting the predicted unconditional noise from the conditional noise:

$$\tilde{\epsilon}_{\theta}(x_t, c, t, \lambda) = \epsilon_{\theta}(x_t, c, t) + \lambda(\epsilon_{\theta}(x_t, c, t) - \epsilon(x_t, \phi, t))$$
(3)

Here $\epsilon_{\theta}(x_t,c,t)$ is the conditional noise satisfying $\mu_{\theta}(x_t,t,c)=\frac{1}{\sqrt{\alpha_t}}(x_t-\frac{\beta_t}{\sqrt{1-\alpha_t}}\epsilon_{\theta}(x_t,c,t))$, where $\alpha_t=1-\beta_t, \bar{\alpha_t}=\prod_{i=1}^t\alpha_i$ (Ho et al., 2020). ϕ refers to no condition during the denoising process.

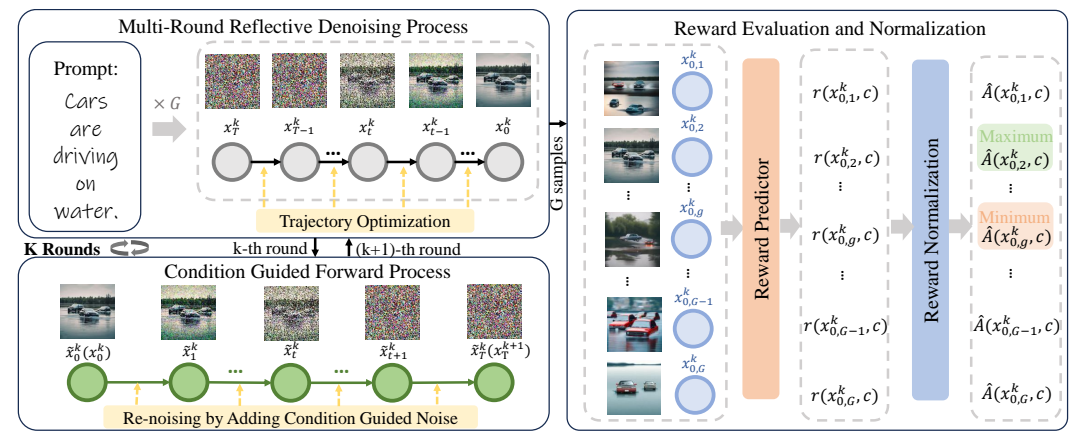


Figure 2: Overview of SRRL. SRRL includes two processes: multi-round reflective denoising process and condition guided forward process. These two processes are repeated for K rounds.

The goal of DDPMs is approximating $q_0(x_0|c)$ with $p_{\theta}(x_0|c) = \int p_{\theta}(x_{0:T}|c)dx_{1:T}$. The denoising process can be seen as a multi-step MDP $\tau = (s_T, a_T, s_{T-1}, a_{T-1}, \cdots, s_0, a_0)$:

$$s_{t} = (c, t, x_{t}), \qquad a_{t} = x_{t-1}, \qquad \pi_{\theta}(a_{t}|s_{t}) = p_{\theta}(x_{t-1}|x_{t}, c), \qquad R(s_{t}, a_{t}) = \begin{cases} r(x_{0}, c), & \text{if } t = 0\\ 0, & \text{otherwise} \end{cases}$$

where s_t is the state at each timestep, a_t is the action to denoise x_t to x_{t-1} , π_{θ} defines the action selection strategy, and R is the reward, which is given by models or human preferences. Therefore, the diffusion denoising process can be viewed as an RL task in which diffusion models act as agents to make decisions (denoising process). The goal of RL is to maximize the expected cumulative reward over the diffusion denoising trajectories sampled from the policy, which can be formulated as:

$$\mathcal{J}_{RL}(\theta) = \mathbb{E}_{c \sim p(c), x_0 \sim p_{\theta}(x_0|c)}[r(x_0, c)] \tag{4}$$

where p(c) is the distribution of text descriptions of images.

3.1.2 Self-Reflective Reinforcement Learning

Existing reinforcement learning algorithms (Black et al., 2023; Fan et al., 2023; Hu et al., 2025) optimize only a single denoising trajectory and can only utilize outcome reward models (ORMs) without reflective reasoning capabilities. Different from them, SRRL aims to optimize the cumulative denoising trajectory, enabling it to utilize process reward models (PRMs) from intermediate results, which enables self-reflective reasoning process. The objective of SRRL is:

$$\mathcal{J}_{SRRL}(\theta) = \mathbb{E}_{c \sim p(c), x_0 \sim p_{\theta}(x_0|c), k \sim U(0, K)}[r(x_0^k, c)] \tag{5}$$

where k refers to the k-th iteration of the reflection process, x_0^k refers to the k-th intermediate sample for evaluation, U refers to uniform distribution. SRRL includes multi-round reflective denoising process and condition guided forward process, which will be detailed in the following sections.

3.2 Multi-Round Reflective Denoising Process

Diffusion models suffer from the issue that reward prediction is limited to final images, preventing the introduction of PRMs and resulting in a lack of reflection capability. To address the issue, SRRL incorporates multiple rounds of RL optimization in the denoising process, providing PRMs and aiming to endow the model with self-reflection capability. Specifically, after each round of the denoising process, SRRL evaluates intermediate images using reward models, which provide process rewards for the entire multi-round process. In the subsequent rounds, SRRL optimizes the trajectory based on the intermediate rewards from previous rounds.

SRRL leverages policy gradient estimation by computing likelihoods and gradients of likelihoods:

$$\nabla_{\theta} \mathcal{J}_{SRRL} = \mathbb{E}_{c \sim p(c), x_0 \sim p_{\theta}(x_0|c), k \sim U(0, K)} [\sum_{t=0}^{T_k} \nabla_{\theta} \log p_{\theta}(x_{t-1}^k | x_t^k, c) r(x_0^k, c)]$$
 (6)

Evaluation of the above requires sampling from the multi-round denoising process, which can be seen as a long MDP $\tau_{SRRL} = (s_T^0, a_T^0, \cdots, s_0^0, a_0^0, \cdots, s_T^k, a_T^k, \cdots, s_0^k, a_0^k, \cdots, s_0^K, a_0^K)$. The reward includes process rewards of intermediate samples: $R(s_t^k, a_t^k) = \begin{cases} r(x_0^k, c), & \text{if } t = 0 \\ 0, & \text{otherwise} \end{cases}$.

We apply Proximal Policy Optimization (PPO) (Schulman et al., 2017) algorithm, including importance sampling and clipping. Besides, we use reward normalization and remove the value function, similar to Group Relative Policy Optimization (Shao et al., 2024) algorithm, and contrastive sampling (Mikolov et al., 2013) is introduced. The PPO update objective is:

$$\nabla_{\theta} \mathbb{E}_{c \sim p(c), k \sim U(0, K)} \frac{1}{G_c} \sum_{i=1}^{G_c} \left(\sum_{t=1}^{T} \left[\min(\frac{p_{\theta}(x_{t-1}^k | x_t^k, c)}{p_{old}(x_{t-1}^k | x_t^k, c)} \hat{A}_i^k, \text{clip}(\frac{p_{\theta}(x_{t-1}^k | x_t^k, c)}{p_{old}(x_{t-1}^k | x_t^k, c)}, 1 - \epsilon, 1 + \epsilon) \hat{A}_i^k) \right) \right)$$

where G_c is the number of remaining samples after contrastive sampling (selecting the maximum and minimum reward values). \hat{A}^k_i is calculated through reward normalization: $\hat{A}^k_i = \frac{r(x^0_{0,i},c)-\max(\{r(x^0_{0,1},c),\cdots,r(x^0_{0,G},c)\})}{\operatorname{std}(\{r(x^0_{0,1},c),\cdots,r(x^0_{0,G},c)\})}$, where G is the number of samples before contrastive sampling and k is the k-th reflection round.

3.3 CONDITION GUIDED FORWARD PROCESS

By optimizing multi-round denoising process, SRRL gains self-reflection ability through PRMs. However, a problem is how to connect the multiple rounds of denoising processes, allowing reflective iteration between image CoT steps. To achieve multi-round self-reflection between different denoising trajectories, SRRL proposes condition guided forward process, which adds conditional noise to intermediate samples at the end of each denoising round to obtain noisy samples for the next round of reflective denoising process.

Given the intermediate sample x_0^k , the condition guided forward process aims to add noise to obtain the noisy sample x_T^{k+1} of the next round, which can be formulated as:

$$x_{T}^{k+1} = \prod_{t=1}^{T} \chi(\tilde{x}_{t}^{k} | \tilde{x}_{t-1}^{k}, c), \quad k = 0, 1, \cdots, K$$

$$\chi(\tilde{x}_{t}^{k} | \tilde{x}_{t-1}^{k}, c) = \sqrt{\frac{\alpha_{t}}{\bar{\alpha}_{t-1}}} \tilde{x}_{t-1}^{k} + (\frac{1 - \alpha_{t}}{\sqrt{1 - \bar{\alpha}_{t}}} - \sqrt{\frac{\alpha_{t}(1 - \bar{\alpha}_{t-1})}{\bar{\alpha}_{t-1}}}) \tilde{\epsilon}_{\theta}(\tilde{x}_{t-1}^{k}, c, t, \lambda)$$
(7)

where $x_T^{k+1} = \tilde{x}_T^k$ and $x_0^k = \tilde{x}_0^k$. SRRL sets CFG guidance scale λ in forward process smaller than that in denoising process, e.g., 1.0 and 4.5. By creating a guidance gap between forward process and denoising process, SRRL injects text condition during forward process, leading to progressively better results with more reflection rounds. SRRL uses DDIM (Song et al., 2020a) inversion scheduler, which is a deterministic sampling method to precisely inject text conditions.

In summary, SRRL optimizes the denoising trajectory over multiple rounds and introduces intermediate sample reward evaluations, which address the issue that reward prediction is limited to final images. Besides, by introducing condition guided forward process, SRRL establishes inter-trajectory CoT connections, enabling iterative reflection and knowledge transfer across sequential steps. Multiple rounds of the denoising and forward process provide self-reflection ability, facilitating image reasoning generation in diffusion models. The pseudo-codes of training and inference process of SRRL are shown in Algorithm 1 and Algorithm 2.

4 EXPERIMENTS

In this section, we evaluate SRRL's effectiveness in image reasoning generation tasks. We aim to answer the following questions: i) Is it possible to leverage a self-reflective reinforcement learning algorithm to achieve image reasoning generation adhered to physical laws and unconventional physical phenomena? ii) How do generated images include reasoning and thought processes?

4.1 EXPERIMENTAL SETUP

T2I diffusion models. We use Stable Diffusion (SD) v1.4 (Rombach et al., 2022), SD XL (Podell et al., 2023) and SD 3 Medium (Esser et al., 2024) as the backbone diffusion models, which are open-source and widely used for T2I tasks. We perform LoRA (Hu et al., 2022) fine-tuning on U-Net in SD, which is a method that saves GPU memory and accelerates training efficiency. During multi-round reflective denoising process, SRRL uses DDIM (Song et al., 2020a) scheduler. During condition guided forward process, SRRL uses DDIM inversion scheduler. The number of sampling steps is set to 20. The implementation details are shown in Appendix 7.

271 272 273

274

275

276

277

278

279

281

283

284

287 288

289

291

292

293

295

296

297

298

299

300

301

302

303 304

305

306

307

308

309

310

311

312 313

314

315

316

317

318

319

320

321

322

323

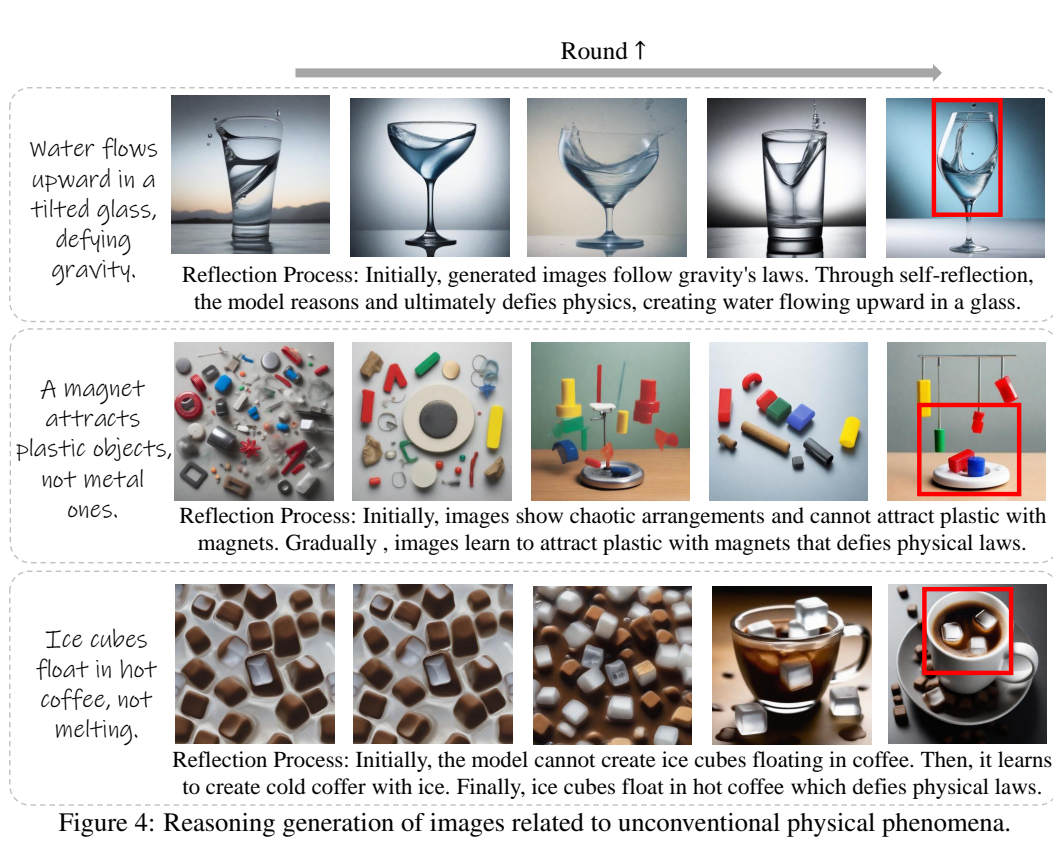
Round 1 Student testing friction with objects on ramps. Reflection Process: Initially, a plank is horizontal with no object on it. Then, objects gradually appear on an inclined plank, enabling a student to explore friction. (related to physical laws) Scientist comparing plant growth with and without Reflection Process: Initially, plants get equal light. Over time, sunlight exposure varies, causing sunlight. height differences—taller with sunlight, shorter without—consistent with biological principles. Person reflecting light using mirrors onto targets. Reflection Process: Initially, mirrors are misshapen or do not reflect light. Later, they reflect light evenly. Eventually, the mirrors reflect light with varying intensity, consistent with optical laws. Figure 3: Reasoning generation of images related to physical laws. **Reward models and metrics.** We use CLIP Score (Hessel et al., 2021), ImageReward (Xu et al.,

2023), and VQAScore (Lin et al., 2024) to evaluate the text-image alignment and image reasoning abilities of models. CLIP Score measures the similarity between text and image embeddings via CLIP model (Radford et al., 2021), trained with contrastive learning for cross-modal alignment. Image reward (Xu et al., 2023) evaluates the general-purpose text-to-image human preference by training on total 137k pairs text-images with expert comparisons. VQAScore (Lin et al., 2024) employs a visual-question-answering model to compute an alignment score. This is achieved by measuring the probability of the model responding 'Yes' to the question: 'Does this figure depict {text}?'. VQAScore is better in evaluating image reasoning ability due to its judgment ability.

Prompt type. We evaluate the effectiveness of our algorithm on three types of prompts, i) Following previous works (Black et al., 2023; Hu et al., 2025), we use the prompt template "a(n) [animal] [activity]", which evaluates text-image alignment. There are 45 kinds of animals and three activities: "riding a bike", "playing chess", and "washing dishes". Animals and activities are randomly matched. ii) Physical phenomenon-related prompts. These prompts include knowledge about physical laws. Details are shown in Appendix 11. iii) Unconventional physical phenomena prompts. These prompts contradict common phenomena to evaluate models' imagination capabilities. Details are shown in Appendix 11. It is worth noting that image reasoning capability and image-text alignment are not equivalent, and we discuss it in Sec. 5.

4.2 PHYSICAL LAW RELATED IMAGE GENERATION

We train models with the SRRL algorithm using prompts related to physical phenomena. Fig. 3 shows some qualitative results. The first prompt is "Student testing friction with objects on ramps". Initially, generated images lack inclined planks, and objects on the plank are unclear. With iterative self-reflection training, the final image includes an inclined plank with clear objects on it, depicting a student testing friction. The second prompt is "Scientist comparing plant growth with and without sunlight", which contains biological principles: plants receiving adequate sunlight grow better than those that do not. At first, two plants are similar. Gradually, the model learns to differentiate the intensity of light exposure on plants. Eventually, the model realizes that plants exposed to more light grow better. The third prompt is "Person reflecting light using mirrors onto targets". It indicates that the light on different mirrors is different. Initially, the mirrors are misshapen or do not reflect any light. Later, they reflect light evenly. Eventually, the mirrors reflect light with varying intensity,



consistent with physical laws. The above results indicate that SRRL, through self-reflection, can gradually learn to reason and generate images following physical laws.

4.3 Unconventional Image Generation

We train models with SRRL algorithm using prompts for unconventional physical phenomena, which are counterintuitive and contradict usual physical phenomena. Some qualitative results are shown in Fig. 4. The first prompt is "Water flows upward in a tilted glass, defying gravity". At first, generated images obey physical laws of gravity. As the self-reflection process continues, the model engages in reasoning and eventually overcomes physical laws, generating an image of water flowing upwards in a glass. The second prompt is "A magnet attracts plastic objects, not metal ones". Initially, the objects in the images are chaotic, indicating that the model does not know how to use a magnet to attract plastic objects. Through self-reflection process, the model learns to attract plastic objects with a magnet, even though this defies physical laws. The third prompt is "Ice cubes float in hot coffee, not melting". The model initially cannot generate ice cubes floating in hot coffee. As the reasoning process progresses, the model learns this concept. From the bubbling coffee in the image, it can be inferred that the coffee is hot, while the ice cubes in the coffee have not melted. From the results above, it can be observed that initially, the model either adheres to physical laws or lacks relevant knowledge. As self-reflection activates its reasoning abilities, the model is able to generate images that defy common sense or physical laws.

4.4 VISUALIZATION OF IMAGE REASONING PROCESS

To visualize the reasoning process of SRRL, we incorporate two prompts: "Draw a balance. The object on the left side is lighter than that on the right side, but the balance leans to the left" and "Cars are driving on water", which contains contradictory knowledge. Reasoning process visualizations of the prompt related to the balance is shown in Fig. 5. We train SD XL model (Podell et al., 2023) with SRRL algorithm on one prompt each time and we use ImageReward (Xu et al., 2023) as the reward model. For results of the first prompt in Fig. 5, initially, the model generates images of a balance either tilted left with no objects or tilted right with lighter objects on the left and heavier ones on the right, both aligning with common sense or physical laws. Eventually, the model produces an image with contradictory elements: the balance is tilted left despite having no objects on the left and a small ball on the right. More reasoning process visualization and analysis are shown in Appendix 10. This

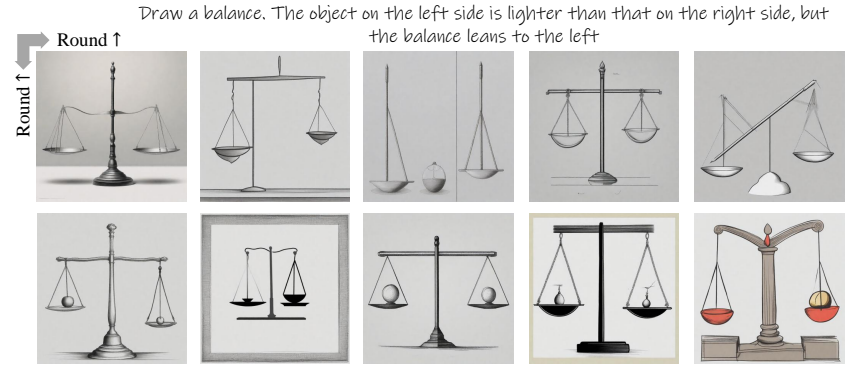


Figure 5: Reasoning generation process of the prompt related to a balance. Initially, the model generates an image of a balance tilted left without objects or tilted right with lighter objects on the left and heavier ones on the right, both following physical laws. Eventually, it learns to create images defying logic: a balance tilts left with no objects on the left and a small ball on the right.



Figure 6: Example of generated images of physical phenomenon related prompts and unconventional physical phenomena prompts by advanced T2I models and SRRL.

suggests that by introducing self-reflection mechanism, SRRL performs reasoning and can generate images adhering to contradictory common sense, showing the model's imagination ability.

4.5 COMPARATIVE ANALYSIS AND ABLATION STUDY

Comparison with Advanced T2I Models. We compare samples of SRRL with those of GPT-4o (Hurst et al., 2024), Qwen-Image (Wu et al., 2025), and Nano-Banana (Fortin et al., 2025), which are most advanced T2I models recently in Fig. 6. SRRL generates similar or higher quality images compared to other advanced models, showing reasoning capabilities akin to other models.

Evaluation of SRRL on Physical-Law and Unconventional Prompts. We evaluate the SRRL algorithm using prompts related to physical laws and unconventional phenomena. The results are presented in Table 1. In comparison to vanilla Stable Diffusion (SD) and DDPO (Black et al., 2023), SRRL consistently achieves superior performance across various reward models.

Comparison on "Animal–Activity" Prompts with Prior Works. We also train SD v1.4 model using SRRL algorithm on the prompt template "a(n) [animal] [activity]" to compare with previous works (Black et al., 2023; Hu et al., 2025). Quantitative results of prompt template "a(n) [animal] [activity]" are shown in Tab. 2. Compared with baseline, SRRL performs better in ImageReward and VQAScore. Appendix 9 shows some qualitative results of the prompt template. Compared to

432 3

Table 1: Quantitative results on physical laws and unconventional phenomena.

4	3	3
4	3	4
4	3	5
4	3	6
4	3	7
4	3	8

_
R
_
S
S
S
_
S
S
S
_
S
S

440 441 442 443



447 448



454 455 456

457 458

453

459 460 461 462 463

464 465 466 467 468 469

470 471

472 473 474

475 476

483

484

485

Image Type **Physical Laws** Unconventional Phenomena CLIPScore CLIPScore eward Models VQAScore ImageReward ImageReward VOAScore D v1.4 (w/o RL) 0.302 0.281 0.559 0.296 0.275 0.520 D v1.4+DDPO 0.321 0.297 0.628 0.321 0.318 0.562 D v1.4+SRRL 0.385 (+27.5%) 0.369 (+31.3%) 0.623 (+11.4%) 0.329 (+11.1%) 0.327 (+18.9%) 0.584 (+12.3%) D XL (w/o RL) 0.326 0.2930.591 0.301 0.2870.544 D XL+DDPO 0.339 0.305 0.637 0.330 0.323 0.589 D XL+SRRL 0.349 (+7.1%) 0.324 (+10.6%) 0.655 (+7.8%) 0.335 (+11.3%) 0.331 (+15.3%) 0.632 (+16.2%) D 3 (w/o RL) 0.357 0.311 0.613 0.339 0.315 0.610 D 3+DDPO 0.372 0.345 0.329 0.626 0.3390.6480.371 (+17.7%) SD 3+SRRL 0.413 (+15.7%)0.368 (+18.3%)0.689 (+12.4%) 0.397 (+17.1%) 0.674 (+10.5%)

Table 2: Quantitative results of the prompt template "a(n) [animal] [activity]".

Methods	SD v1.4	DDPO (Black et al., 2023)	B2-DiffuRL (Hu et al., 2025)	SRRL (Ours)
CLIP Score ↑	0.3624	0.3683	0.3674	0.3662
ImageReward ↑	0.2823	0.3534	0.3682	0.3807
VQAScore ↑	0.6045	0.6145	0.6174	0.6338

baselines, SRRL generates images that are more prompt-aligned and of higher quality, indicating that self-reflection mechanism also enhances models' text-to-image alignment ability.

Reflection Rounds and Refinement in Image Generation. We assess the performance of SRRL across prompts concerning physical phenomena and unconventional physical scenarios, with respect to the increasing number of reflection rounds, and results are shown in Fig. 7. The quality of generated images improves as the round increases with self-reflection process. We also notice the phenomenon of reflection refinement, which involves adjusting the generated images through image reconstruction.

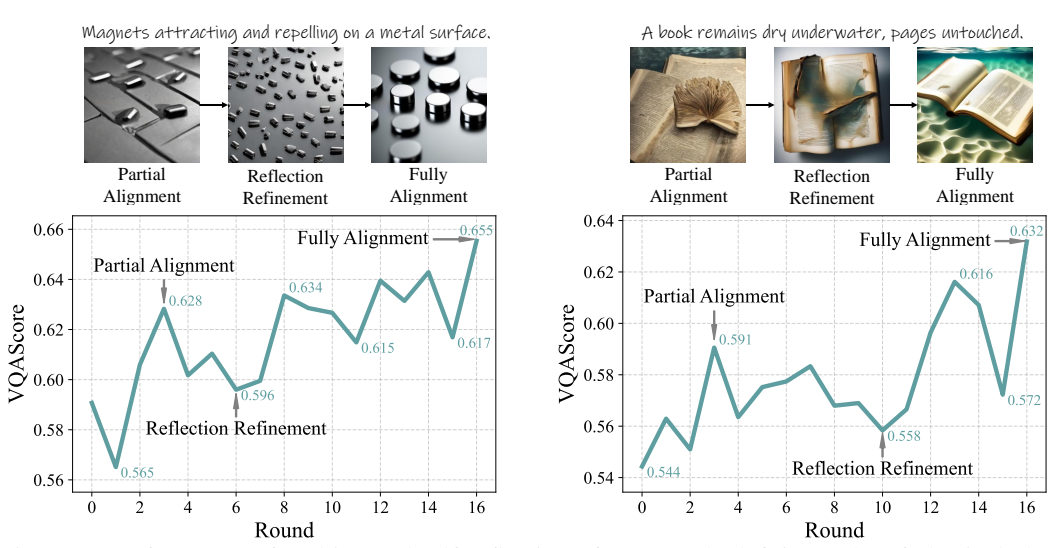


Figure 7: Performance of multi-round self-reflection of SRRL. The left is results of physical phenomenon related prompts, and the right is those of unconventional physical phenomena prompts. The figure above shows some cases of reflection process. All experiments are done based on SD XL.

5 DISCUSSION AND CONCLUSION

Chain-of-thought (CoT) has recently been applied to LLMs to enhance self-reflection in complex tasks. Extending CoT to image generation raises the question of which challenges it should address. We focus on generating images consistent with physical laws, as this setting highlights models' reasoning and imaginative capacity. Unlike text-image alignment, adherence to physical laws is difficult because such constraints are often implicit in textual prompts.

We introduce SRRL, a self-reflective reinforcement learning algorithm for diffusion models that incorporates image CoT and multi-round reflective denoising with condition-guided forward processes. Experiments demonstrate that SRRL produces images consistent with physical laws and unconventional scenarios, thereby advancing image reasoning.

REFERENCES

- Lichen Bai, Shitong Shao, Zikai Zhou, Zipeng Qi, Zhiqiang Xu, Haoyi Xiong, and Zeke Xie. Zigzag diffusion sampling: Diffusion models can self-improve via self-reflection. In *The Thirteenth International Conference on Learning Representations*, volume 2, 2024.
- Kevin Black, Michael Janner, Yilun Du, Ilya Kostrikov, and Sergey Levine. Training diffusion models with reinforcement learning. *arXiv preprint arXiv:2305.13301*, 2023.
- Arwen Bradley and Preetum Nakkiran. Classifier-free guidance is a predictor-corrector. *arXiv* preprint arXiv:2408.09000, 2024.
- Hyungjin Chung, Jeongsol Kim, Geon Yeong Park, Hyelin Nam, and Jong Chul Ye. Cfg++: Manifold-constrained classifier free guidance for diffusion models. *arXiv preprint arXiv:2406.08070*, 2024.
- Prafulla Dhariwal and Alexander Nichol. Diffusion models beat gans on image synthesis. *Advances in neural information processing systems*, 34:8780–8794, 2021.
- Patrick Esser, Sumith Kulal, Andreas Blattmann, Rahim Entezari, Jonas Müller, Harry Saini, Yam Levi, Dominik Lorenz, Axel Sauer, Frederic Boesel, et al. Scaling rectified flow transformers for high-resolution image synthesis. In *Forty-first international conference on machine learning*, 2024.
- Ying Fan, Olivia Watkins, Yuqing Du, Hao Liu, Moonkyung Ryu, Craig Boutilier, Pieter Abbeel, Mohammad Ghavamzadeh, Kangwook Lee, and Kimin Lee. Dpok: Reinforcement learning for fine-tuning text-to-image diffusion models. *Advances in Neural Information Processing Systems*, 36:79858–79885, 2023.
- Alisa Fortin, Guillaume Vernade, Kat Kampf, and Ammaar Reshi. Introducing gemini 2.5 flash image, our state-of-the-art image model, August 2025. URL https://developers.googleblog.com/en/introducing-gemini-2-5-flash-image/.
- Daya Guo, Dejian Yang, Haowei Zhang, Junxiao Song, Ruoyu Zhang, Runxin Xu, Qihao Zhu, Shirong Ma, Peiyi Wang, Xiao Bi, et al. Deepseek-r1: Incentivizing reasoning capability in llms via reinforcement learning. *arXiv preprint arXiv:2501.12948*, 2025a.
- Ziyu Guo, Renrui Zhang, Chengzhuo Tong, Zhizheng Zhao, Peng Gao, Hongsheng Li, and Pheng-Ann Heng. Can we generate images with cot? let's verify and reinforce image generation step by step. *arXiv preprint arXiv:2501.13926*, 2025b.
- Jack Hessel, Ari Holtzman, Maxwell Forbes, Ronan Le Bras, and Yejin Choi. Clipscore: A reference-free evaluation metric for image captioning. *arXiv preprint arXiv:2104.08718*, 2021.
- Jonathan Ho and Tim Salimans. Classifier-free diffusion guidance. *arXiv preprint arXiv:2207.12598*, 2022.
- Jonathan Ho, Ajay Jain, and Pieter Abbeel. Denoising diffusion probabilistic models. *Advances in neural information processing systems*, 33:6840–6851, 2020.
- Edward J Hu, Yelong Shen, Phillip Wallis, Zeyuan Allen-Zhu, Yuanzhi Li, Shean Wang, Lu Wang, Weizhu Chen, et al. Lora: Low-rank adaptation of large language models. *ICLR*, 1(2):3, 2022.
- Zijing Hu, Fengda Zhang, Long Chen, Kun Kuang, Jiahui Li, Kaifeng Gao, Jun Xiao, Xin Wang, and Wenwu Zhu. Towards better alignment: Training diffusion models with reinforcement learning against sparse rewards. *arXiv preprint arXiv:2503.11240*, 2025.
- Kaiyi Huang, Kaiyue Sun, Enze Xie, Zhenguo Li, and Xihui Liu. T2i-compbench: A comprehensive benchmark for open-world compositional text-to-image generation. *Advances in Neural Information Processing Systems*, 36:78723–78747, 2023.
- Wenxuan Huang, Bohan Jia, Zijie Zhai, Shaosheng Cao, Zheyu Ye, Fei Zhao, Zhe Xu, Yao Hu, and Shaohui Lin. Vision-r1: Incentivizing reasoning capability in multimodal large language models. *arXiv* preprint arXiv:2503.06749, 2025.

- Binyuan Hui, Jian Yang, Zeyu Cui, Jiaxi Yang, Dayiheng Liu, Lei Zhang, Tianyu Liu, Jiajun Zhang, Bowen Yu, Keming Lu, et al. Qwen2. 5-coder technical report. *arXiv preprint arXiv:2409.12186*, 2024.
- Aaron Hurst, Adam Lerer, Adam P Goucher, Adam Perelman, Aditya Ramesh, Aidan Clark, AJ Ostrow, Akila Welihinda, Alan Hayes, Alec Radford, et al. Gpt-4o system card. *arXiv preprint arXiv:2410.21276*, 2024.
 - Aaron Jaech, Adam Kalai, Adam Lerer, Adam Richardson, Ahmed El-Kishky, Aiden Low, Alec Helyar, Aleksander Madry, Alex Beutel, Alex Carney, et al. Openai o1 system card. arXiv preprint arXiv:2412.16720, 2024.
 - Naman Jain, King Han, Alex Gu, Wen-Ding Li, Fanjia Yan, Tianjun Zhang, Sida Wang, Armando Solar-Lezama, Koushik Sen, and Ion Stoica. Livecodebench: Holistic and contamination free evaluation of large language models for code. *arXiv* preprint arXiv:2403.07974, 2024.
 - Dongzhi Jiang, Guanglu Song, Xiaoshi Wu, Renrui Zhang, Dazhong Shen, Zhuofan Zong, Yu Liu, and Hongsheng Li. Comat: Aligning text-to-image diffusion model with image-to-text concept matching. *Advances in Neural Information Processing Systems*, 37:76177–76209, 2024.
 - Dongzhi Jiang, Ziyu Guo, Renrui Zhang, Zhuofan Zong, Hao Li, Le Zhuo, Shilin Yan, Pheng-Ann Heng, and Hongsheng Li. T2i-r1: Reinforcing image generation with collaborative semantic-level and token-level cot. *arXiv preprint arXiv:2505.00703*, 2025a.
 - Dongzhi Jiang, Renrui Zhang, Ziyu Guo, Yanwei Li, Yu Qi, Xinyan Chen, Liuhui Wang, Jianhan Jin, Claire Guo, Shen Yan, et al. Mme-cot: Benchmarking chain-of-thought in large multimodal models for reasoning quality, robustness, and efficiency. *arXiv preprint arXiv:2502.09621*, 2025b.
 - Diederik P Kingma and Jimmy Ba. Adam: A method for stochastic optimization. *arXiv preprint arXiv:1412.6980*, 2014.
 - Tiancheng Li, Weijian Luo, Zhiyang Chen, Liyuan Ma, and Guo-Jun Qi. Self-guidance: Boosting flow and diffusion generation on their own. *arXiv* preprint arXiv:2412.05827, 2024.
 - Hunter Lightman, Vineet Kosaraju, Yuri Burda, Harrison Edwards, Bowen Baker, Teddy Lee, Jan Leike, John Schulman, Ilya Sutskever, and Karl Cobbe. Let's verify step by step. In *The Twelfth International Conference on Learning Representations*, 2023.
 - Zhiqiu Lin, Deepak Pathak, Baiqi Li, Jiayao Li, Xide Xia, Graham Neubig, Pengchuan Zhang, and Deva Ramanan. Evaluating text-to-visual generation with image-to-text generation. In *European Conference on Computer Vision*, pp. 366–384. Springer, 2024.
 - Pan Lu, Hritik Bansal, Tony Xia, Jiacheng Liu, Chunyuan Li, Hannaneh Hajishirzi, Hao Cheng, Kai-Wei Chang, Michel Galley, and Jianfeng Gao. Mathvista: Evaluating math reasoning in visual contexts with gpt-4v, bard, and other large multimodal models. *CoRR*, 2023.
 - Zhiyuan Ma, Guoli Jia, Biqing Qi, and Bowen Zhou. Safe-sd: Safe and traceable stable diffusion with text prompt trigger for invisible generative watermarking. In *ACM Multimedia* 2024.
 - Zhiyuan Ma, Guoli Jia, and Bowen Zhou. Adapedit: Spatio-temporal guided adaptive editing algorithm for text-based continuity-sensitive image editing. In *Proceedings of the AAAI Conference on Artificial Intelligence*, volume 38, pp. 4154–4161, 2024.
- Navonil Majumder, Chia-Yu Hung, Deepanway Ghosal, Wei-Ning Hsu, Rada Mihalcea, and Soujanya Poria. Tango 2: Aligning diffusion-based text-to-audio generations through direct preference optimization. In *Proceedings of the 32nd ACM International Conference on Multimedia*, pp. 564–572, 2024.
- Fanqing Meng, Lingxiao Du, Zongkai Liu, Zhixiang Zhou, Quanfeng Lu, Daocheng Fu, Tiancheng Han, Botian Shi, Wenhai Wang, Junjun He, et al. Mm-eureka: Exploring the frontiers of multimodal reasoning with rule-based reinforcement learning. *arXiv* preprint arXiv:2503.07365, 2025.

- Tomas Mikolov, Ilya Sutskever, Kai Chen, Greg S Corrado, and Jeff Dean. Distributed representations of words and phrases and their compositionality. *Advances in neural information processing systems*, 26, 2013.
- Chong Mou, Xintao Wang, Liangbin Xie, Yanze Wu, Jian Zhang, Zhongang Qi, and Ying Shan. T2i-adapter: Learning adapters to dig out more controllable ability for text-to-image diffusion models. In *Proceedings of the AAAI Conference on Artificial Intelligence*, volume 38, pp. 4296–4304, 2024.
- Alexander Quinn Nichol and Prafulla Dhariwal. Improved denoising diffusion probabilistic models. In *International conference on machine learning*, pp. 8162–8171. PMLR, 2021.
- Long Ouyang, Jeffrey Wu, Xu Jiang, Diogo Almeida, Carroll Wainwright, Pamela Mishkin, Chong Zhang, Sandhini Agarwal, Katarina Slama, Alex Ray, et al. Training language models to follow instructions with human feedback. *Advances in neural information processing systems*, 35:27730–27744, 2022.
- Dustin Podell, Zion English, Kyle Lacey, Andreas Blattmann, Tim Dockhorn, Jonas Müller, Joe Penna, and Robin Rombach. Sdxl: Improving latent diffusion models for high-resolution image synthesis. *arXiv preprint arXiv:2307.01952*, 2023.
- Alec Radford, Jong Wook Kim, Chris Hallacy, Aditya Ramesh, Gabriel Goh, Sandhini Agarwal, Girish Sastry, Amanda Askell, Pamela Mishkin, Jack Clark, et al. Learning transferable visual models from natural language supervision. In *International conference on machine learning*, pp. 8748–8763. PmLR, 2021.
- Aditya Ramesh, Mikhail Pavlov, Gabriel Goh, Scott Gray, Chelsea Voss, Alec Radford, Mark Chen, and Ilya Sutskever. Zero-shot text-to-image generation. In *International conference on machine learning*, pp. 8821–8831. Pmlr, 2021.
- Aditya Ramesh, Prafulla Dhariwal, Alex Nichol, Casey Chu, and Mark Chen. Hierarchical text-conditional image generation with clip latents. *arXiv preprint arXiv:2204.06125*, 1(2):3, 2022.
- Allen Z Ren, Justin Lidard, Lars L Ankile, Anthony Simeonov, Pulkit Agrawal, Anirudha Majumdar, Benjamin Burchfiel, Hongkai Dai, and Max Simchowitz. Diffusion policy policy optimization. *arXiv preprint arXiv:2409.00588*, 2024.
- Robin Rombach, Andreas Blattmann, Dominik Lorenz, Patrick Esser, and Björn Ommer. High-resolution image synthesis with latent diffusion models. In *Proceedings of the IEEE/CVF conference on computer vision and pattern recognition*, pp. 10684–10695, 2022.
- Nataniel Ruiz, Yuanzhen Li, Varun Jampani, Yael Pritch, Michael Rubinstein, and Kfir Aberman. Dreambooth: Fine tuning text-to-image diffusion models for subject-driven generation. In *Proceedings of the IEEE/CVF Conference on Computer Vision and Pattern Recognition*, pp. 22500–22510, 2023.
- Chitwan Saharia, William Chan, Saurabh Saxena, Lala Li, Jay Whang, Emily L Denton, Kamyar Ghasemipour, Raphael Gontijo Lopes, Burcu Karagol Ayan, Tim Salimans, et al. Photorealistic text-to-image diffusion models with deep language understanding. *Advances in neural information processing systems*, 35:36479–36494, 2022.
- John Schulman, Filip Wolski, Prafulla Dhariwal, Alec Radford, and Oleg Klimov. Proximal policy optimization algorithms. *arXiv preprint arXiv:1707.06347*, 2017.
- Zhihong Shao, Peiyi Wang, Qihao Zhu, Runxin Xu, Junxiao Song, Xiao Bi, Haowei Zhang, Mingchuan Zhang, YK Li, Y Wu, et al. Deepseekmath: Pushing the limits of mathematical reasoning in open language models. *arXiv preprint arXiv:2402.03300*, 2024.
- Jiaming Song, Chenlin Meng, and Stefano Ermon. Denoising diffusion implicit models. *arXiv* preprint arXiv:2010.02502, 2020a.
- Yang Song and Stefano Ermon. Improved techniques for training score-based generative models. *Advances in neural information processing systems*, 33:12438–12448, 2020.

- Yang Song, Jascha Sohl-Dickstein, Diederik P Kingma, Abhishek Kumar, Stefano Ermon, and Ben Poole. Score-based generative modeling through stochastic differential equations. *arXiv* preprint *arXiv*:2011.13456, 2020b.
- Bram Wallace, Meihua Dang, Rafael Rafailov, Linqi Zhou, Aaron Lou, Senthil Purushwalkam, Stefano Ermon, Caiming Xiong, Shafiq Joty, and Nikhil Naik. Diffusion model alignment using direct preference optimization. In *Proceedings of the IEEE/CVF Conference on Computer Vision and Pattern Recognition*, pp. 8228–8238, 2024.
- Jason Wei, Xuezhi Wang, Dale Schuurmans, Maarten Bosma, Fei Xia, Ed Chi, Quoc V Le, Denny Zhou, et al. Chain-of-thought prompting elicits reasoning in large language models. *Advances in neural information processing systems*, 35:24824–24837, 2022.
- Chenfei Wu, Jiahao Li, Jingren Zhou, Junyang Lin, Kaiyuan Gao, Kun Yan, Sheng-ming Yin, Shuai Bai, Xiao Xu, Yilei Chen, et al. Qwen-image technical report. *arXiv preprint arXiv:2508.02324*, 2025.
- Jiazheng Xu, Xiao Liu, Yuchen Wu, Yuxuan Tong, Qinkai Li, Ming Ding, Jie Tang, and Yuxiao Dong. Imagereward: Learning and evaluating human preferences for text-to-image generation. *Advances in Neural Information Processing Systems*, 36:15903–15935, 2023.
- Yi Yang, Xiaoxuan He, Hongkun Pan, Xiyan Jiang, Yan Deng, Xingtao Yang, Haoyu Lu, Dacheng Yin, Fengyun Rao, Minfeng Zhu, et al. R1-onevision: Advancing generalized multimodal reasoning through cross-modal formalization. *arXiv preprint arXiv:2503.10615*, 2025.
- Lvmin Zhang, Anyi Rao, and Maneesh Agrawala. Adding conditional control to text-to-image diffusion models. In *Proceedings of the IEEE/CVF International Conference on Computer Vision*, pp. 3836–3847, 2023.
- Renrui Zhang, Xinyu Wei, Dongzhi Jiang, Ziyu Guo, Shicheng Li, Yichi Zhang, Chengzhuo Tong, Jiaming Liu, Aojun Zhou, Bin Wei, et al. Mavis: Mathematical visual instruction tuning with an automatic data engine. *arXiv preprint arXiv:2407.08739*, 2024.

6 DERIVATIONS

6.1 EQUATION 6

$$\begin{split} \nabla_{\theta}[-\mathcal{J}_{SRRL}(\theta)] &= \nabla_{\theta} \mathbb{E}_{p(c)} \mathbb{E}_{p_{\theta}(x_{0}|c)} \mathbb{E}_{k \sim U(0,K)}[-r(x_{0}^{k},c)] \\ &= -\mathbb{E}_{p(c)} \mathbb{E}_{k \sim U(0,K)} [\nabla_{\theta} \int r(x_{0}^{k},c) p_{\theta}(x_{0}^{k}|c) dx_{0}^{k}] \\ &= -\mathbb{E}_{p(c)} \mathbb{E}_{k \sim U(0,K)} [\nabla_{\theta} \int r(x_{0}^{k},c) (\int p_{\theta}(x_{0:T}^{k}|c) dx_{1:T}^{k}) dx_{0}^{k}] \\ &= -\mathbb{E}_{p(c)} \mathbb{E}_{k \sim U(0,K)} [\int \nabla_{\theta} \log p_{\theta}(x_{0:T}^{k}|c) r(x_{0}^{k},c) p_{\theta}(x_{0:T}^{k}|c) dx_{0:T}^{k}] \\ &= -\mathbb{E}_{p(c)} \mathbb{E}_{k \sim U(0,K)} [\int \nabla_{\theta} \log \left(p_{T}(x_{T}^{k}|c) \prod_{t=1}^{T} p_{\theta}(x_{t-1}^{k}|x_{t}^{k},c) \right) r(x_{0}^{k},c) p_{\theta}(x_{0:T}^{k}|c) dx_{0:T}^{k}] \\ &= -\mathbb{E}_{p(c)} \mathbb{E}_{p_{\theta}(x_{0:T}^{k}|c)} \mathbb{E}_{k \sim U(0,K)} [\sum_{t=1}^{T} \nabla_{\theta} \log p_{\theta}(x_{t-1}^{k}|x_{t}^{k},c) r(x_{0}^{k},c)] \end{split}$$

Here the proof uses the continuous assumptions of $p_{\theta}(x_{0:T}^k|c)r(x_0^k,c)$.

6.2 EQUATION 7

Following DDPM (Ho et al., 2020), the denoising process is formulated as:

$$x_{t-1}^k = \frac{\sqrt{\bar{\alpha}_{t-1}}}{\sqrt{\alpha_t}} (x_t^k - \frac{1 - \alpha_t}{\sqrt{1 - \bar{\alpha}_t}} \epsilon_{\theta}(x_t^k, c, t, \lambda)) + \sqrt{1 - \bar{\alpha}_{t-1}} \epsilon_{\theta}(x_t^k, c, t, \lambda)$$
(8)

Then, solve for x_t based on x_{t-1} ,

$$\tilde{x}_t^k = \sqrt{\frac{\alpha_t}{\bar{\alpha}_{t-1}}} \tilde{x}_{t-1}^k + \left(\frac{1 - \alpha_t}{\sqrt{1 - \bar{\alpha}_t}} - \sqrt{\frac{\alpha_t (1 - \bar{\alpha}_{t-1})}{\bar{\alpha}_{t-1}}}\right) \tilde{\epsilon}_{\theta}(\tilde{x}_{t-1}^k, c, t, \lambda)$$
(9)

Here we leverage the assumption that $\tilde{\epsilon}_{\theta}(\tilde{x}_{t-1}^k,c,t,\lambda) \approx \tilde{\epsilon}_{\theta}(\tilde{x}_t^k,c,t,\lambda)$.

We can inject condition if there is a guidance gap between forward process and denoising process.

For convenience, we set:

$$\gamma_t = \sqrt{\frac{\alpha_t}{\bar{\alpha}_{t-1}}}, \qquad \eta_t = \left(\frac{1 - \alpha_t}{\sqrt{1 - \bar{\alpha}_t}} - \sqrt{\frac{\alpha_t (1 - \bar{\alpha}_{t-1})}{\bar{\alpha}_{t-1}}}\right) \tag{10}$$

Then,

$$\tilde{x}_{T}^{k} = \gamma_{T} \tilde{x}_{T-1}^{k} + \eta_{T} \tilde{\epsilon}_{\theta} (\tilde{x}_{T-1}^{k}, c, t, \lambda)
= \gamma_{T} \gamma_{T-1} \tilde{x}_{T-2}^{k} + \gamma_{T} \eta_{T-1} \tilde{\epsilon}_{\theta} (\tilde{x}_{T-2}^{k}, c, t, \lambda) + \eta_{T} \tilde{\epsilon}_{\theta} (\tilde{x}_{T-1}^{k}, c, t, \lambda)
= \cdots
= \prod_{i=0}^{T} \gamma_{i} \tilde{x}_{0} + \sum_{t=1}^{T} \eta_{t} \prod_{l=t+1}^{T} \gamma_{l} \epsilon_{\theta} (\tilde{x}_{t-1}^{k}, c, t, \lambda)$$
(11)

Similarly, we can get:

$$x_T^k = \prod_{i=0}^T \gamma_i x_0 + \sum_{t=1}^T \eta_t \prod_{k=t+1}^T \eta_k \epsilon_\theta(x_{t-1}^k, c, t, \lambda_{\text{Forward}})$$
 (12)

The guidance gap can be formulated as:

$$\delta_{k} = (x_{T}^{k} - \tilde{x}_{T}^{k})^{2}$$

$$= \left[\prod_{i=0}^{T} \gamma_{i}(x_{0} - \tilde{x}_{0}) + \sum_{t=1}^{T} \eta_{t} \prod_{l=t+1}^{T} \gamma_{l}(\epsilon_{\theta}(x_{t-1}^{k}, c, t, \lambda_{\text{Forward}}) - \epsilon_{\theta}(\tilde{x}_{t-1}^{k}, c, t, \lambda))\right]^{2}$$

$$= \left(\sum_{t=1}^{T} F(\eta_{t}, \gamma_{t})(\epsilon_{\theta}(x_{t-1}^{k}, c, t, \lambda_{\text{Forward}}) - \epsilon_{\theta}(\tilde{x}_{t-1}^{k}, c, t, \lambda))\right)^{2}$$

$$= \left(\sum_{t=1}^{T} F(\eta_{t}, \gamma_{t})(\lambda_{\text{Forward}} - \lambda)\epsilon_{\theta}(x_{t-1}^{k}, c, t)\right)^{2}$$

$$(13)$$

By setting a guidance scale gap between λ and λ_{Forward} , we can inject text condition during condition injection reflection forward process. Through multiple rounds of self reflection, the effect of condition injection is enhanced.

7 IMPLEMENTATION DETAILS

When fine-tuning Stable Diffusion model (Rombach et al., 2022; Podell et al., 2023) using LoRA according to SRRL algorithm, the configs are:

Config	Value	
LoRA rank	4	
LoRA alpha	4	
lr	1e-4	
optimizer	Adam (Kingma & Ba, 2014)	
weight decay of optimizer	1e-4	
eta_1,eta_2	(0.9, 0.999)	
number of samples per batch G	32	
self-reflection total rounds K	10	
denoising timestep T	20	
reward function r	CLIP Score, ImageReward, VQAScore	
training epoch number E	2	
forward guidance scale	0.5	
denoising guidance scale	3.0	
inference guidance scale	7.5	

PSEUDO-CODE OF SRRL

811 812 813

810

Algorithm 1: SRRL Training Process

```
814
          Input: Pretrained diffusion model p_{\theta}, denoising timestep T, self-reflection total rounds K, number
815
               of samples per batch G, prompts list C, reward function r, training epoch number E.
816
            1: k = 0
817
           2: repeat
818
           3:
                  e = 0
819
           4:
                  repeat
820
           5:
                     SampleList=[]
821
           6:
                     n = 0
822
           7:
                     repeat
823
           8:
                        Random choose prompt c from C,
           9:
                        Random sample Gaussian noise x_T in \mathcal{N}(0,1),
824
          10:
825
          11:
                        repeat
826
          12:
                           Denoise x_T^i to x_0^i with p_\theta,
                           Noise injection x_0^i to x_T^{i+1} with p_\theta,
          13:
828
                           i = i + 1
          14:
829
                        until i = k
          15:
830
          16:
                        x_{T:0}^k = \text{DDIM-Scheduler}_{\theta}(x_T^k \to x_0^k),
831
                        SampleList.append([x_{T\cdot 0}^k,c]),
          17:
832
                        n = n + 1
          18:
833
                     until n = G
          19:
834
                     Evaluate r(x_{0,i=1:G}^k, c),
          20:
835
                     score_{i=1}^{G} = Reward Normalization(r(x_{0,i=1:G}^{k}, c),
          21:
836
          22:
                     score_{max}, i_{max} = maximum(score_{i=1}^{G}), index(score_{max}),
837
                     score_{min}, i_{min} = minimum(score_{i=1}^{G}), index(score_{min}),
          23:
838
                     \text{update } \theta \text{ according to } [x_{T:0,i_{\max}}^k, \text{score}_{\max}, x_{T:0,i_{\min}}^k, \text{score}_{\min}, c].
          24:
839
          25:
                     e = e + 1
840
                  until e = E
          26:
841
                  k = k + 1
          27:
          28: until k = K
843
          Output: Fine-tuned Model p_{\theta'}
844
```

Algorithm 2: SRRL Inference Process

```
Input: Fine-tuned diffusion model p_{\theta}, self-reflection rounds k
 1: Random sample Gaussian noise x_T^0 in \mathcal{N}(0,1),
 2: i = 0
 3: repeat
       Denoise x_T^i to x_0^i with p_\theta,
       Noise injection x_0^i to x_T^{i+1} with p_\theta,
       i = i + 1
 7: until i = k
 8: Denoise x_T^k to x_0^k
Output: Self-reflective images x_0^k
```

845

846

847

848

849

850

851

852

853

854

855

QUALITATIVE COMPARISON ON "ANIMAL-ACTIVITY" PROMPTS

860 861 862

863

Qualitative results on "Animal-Activity" Prompts of SRRL, DDPO (Black et al., 2023), B2-DiffuRL (Hu et al., 2025), and vanilla SD are shown in Fig. 8.

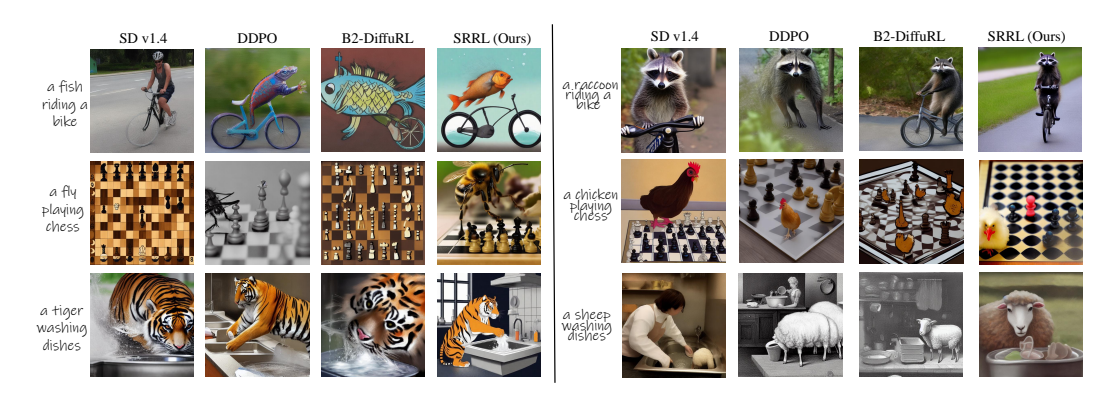


Figure 8: Examples of prompt template "a(n) [animal] [activity]" by baselines (Rombach et al., 2022; Black et al., 2023; Hu et al., 2025) and SRRL.

10 ADDITIONAL VISUALIZATION OF IMAGE REASONING PROCESS

Additional visualization of image reasoning process is shown in Fig. 9. For results of the prompt in Fig. 9, the general common sense is that cars drive on land, but the prompt requires generating an image of a car driving on water. In the initially generated images, the car appears to fly out of the water. In the final generated images, the car drives in the center of the lake rather than floats.

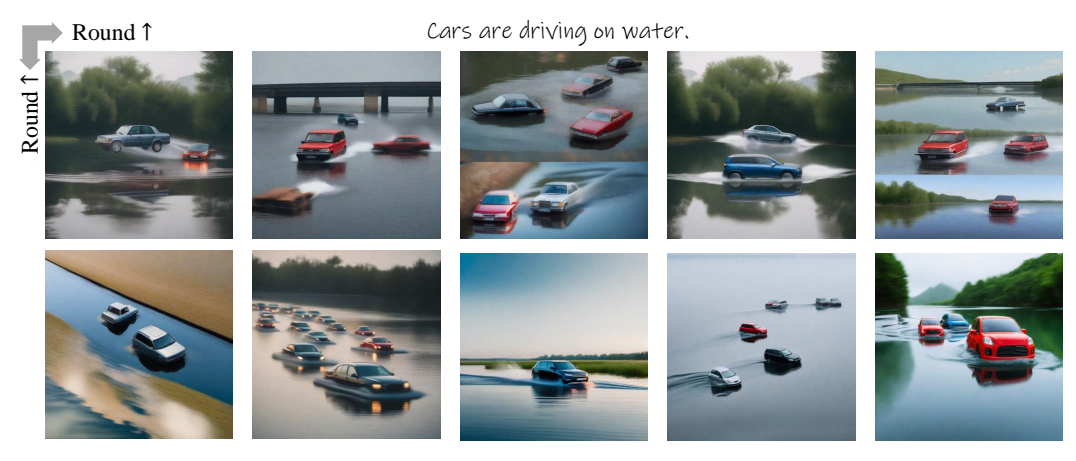


Figure 9: Reasoning generation process of prompt related to cars. Common sense dictates that cars drive on land, but the prompt asks for an image of a car on water. Initially, cars seems to fly out of the water, but in the final images, they drive across the center of the lake rather than float.

11 PROMPT DETAILS

11.1 PROMPTS TEMPLATE "A(N) [ANIMAL] [ACTIVITY]"

Prompts of the template "a(n) [animal] [activity]" are shown in Fig. 10, which are used to evaluate the text-image alignment of SRRL.

11.2 PHYSICAL PHENOMENON RELATED PROMPTS

Physical phenomenon related prompts are shown in Fig. 11, which are used to evaluate the image reasoning ability of SRRL.

919

920

921

922

923

924

925

926

927

928

929

930

931

932

933

934

936

937

938

939

940

941 942

943 944

945

946

947

948

949

950

951

952 953

954

955

956

957

958

959

960

961

962

963 964

965 966

967 968

969

970

971

```
"a cat washing dishes",
                                                        "a fish riding a bike",
  "a dog washing dishes".
                                                        "a shark riding a bike",
                                                        "a whale riding a bike",
 "a horse washing dishes"
"a monkey washing dishes"
                                                       "a dolphin riding a bike"
 "a rabbit washing dishes".
                                                       "a squirrel riding a bike"
 "a zebra washing dishes",
                                                       "a mouse riding a bike",
 "a spider washing dishes"
                                                         "a rat riding a bike",
  "a bird washing dishes".
                                                        "a snake riding a bike"
 "a sheep washing dishes",
                                                        "a turtle playing chess",
  "a deer washing dishes",
                                                        "a frog playing chess",
  "a cow washing dishes".
                                                       "a chicken playing chess"
  "a goat washing dishes",
                                                        "a duck playing chess",
  "a lion washing dishes",
                                                       "a goose playing chess",
  "a tiger washing dishes"
                                                         "a bee playing chess",
  "a bear washing dishes".
                                                         "a pig playing chess",
  "a raccoon riding a bike",
                                                       "a turkey playing chess",
    "a fox riding a bike",
                                                         "a fly playing chess",
   "a wolf riding a bike"
                                                       "a llama playing chess"
   "a lizard riding a bike",
                                                       "a camel playing chess",
   "a beetle riding a bike",
                                                         "a bat playing chess",
    "a ant riding a bike",
                                                       "a gorilla playing chess",
 "a butterfly riding a bike"
                                                     "a hedgehog playing chess",
"a kangaroo playing chess"
                                                      "a kangaroo playing chess"
```

Figure 10: Prompts of the template "a(n) [animal] [activity]".

```
"Dominoes falling to demonstrate cause and effect logic.",
  "Detective connecting clues on a corkboard with string.",
    "Ball rolling down ramp, showing gravity in action.",
    "Magnets attracting and repelling on a metal surface."
      "Student balancing a scale with diverse weights.",
 "Pendulum swinging, illustrating conservation of energy.",
      "Child testing objects' buoyancy in a water tank.",
      "Person decoding a ciphered message on paper.",
"Scientist comparing plant growth with and without sunlight.",
     "Teacher drawing a Venn diagram to explain logic.",
      "Robot sorting colored blocks by shape and hue.",
        "Person solving a Sudoku puzzle on a desk.",
      "Two kids racing toy cars on different surfaces.",
       "Person tracing electrical circuits with a tester.",
"Detective examining fingerprints with a magnifying glass.",
    "Student observing chemical reactions in test tubes.",
     "Person reflecting light using mirrors onto targets."
      "Detective piecing together torn letter fragments.",
      "Person solving a logic puzzle on a chalkboard.".
       "Student testing friction with objects on ramps."
```

Figure 11: Physical phenomenon related prompts.

11.3 Unconventional Physical Phenomena Prompts

Unconventional physical phenomena prompts are shown in Fig. 12, which are used to evaluate the image reasoning ability of SRRL.

Physical phenomenon related prompts and unconventional physical phenomena prompts are provided by GPT-4o. The prompts are: "Please help me think of some prompts generated from images that

 "A ball rolling uphill against gravity, surprising onlookers.", "Dominoes falling in reverse, standing themselves up.", "Detective finds a footprint leading to a floating shoe.", "A magnet attracts plastic objects, not metal ones.", "Shadow points away from the light source, defying logic.", "A plant grows upside down, roots in the air.", "Water flows upward in a tilted glass, defying gravity.", "A clock runs backward, time reversing for everyone.", "A mirror reflects a different object than in front.", "Ice cubes float in hot coffee, not melting.", "A candle flame burns downward, not upward.", "Objects fall slower in a vacuum than in air.", "A book remains dry underwater, pages untouched.", "A person walks through a solid wall unharmed.", "Raindrops fall upward from the ground to the sky.", "A compass needle spins wildly, never settling north.", "A shadow appears without any object present.", "A person lifts a heavy rock effortlessly, surprising others.", "A glass shatters before being touched by the ball.", "A balloon sinks in air, going downwards rapidly."

Figure 12: Unconventional physical phenomena prompts.

demonstrate logical reasoning, in English, and output in JSON format: [prompt1, prompt2,...]. Please provide me with 20 prompts" and "Please help me think of some prompts generated from images that demonstrate reasoning and unconventional phenomena. They should be in English and output in JSON format: [prompt1, prompt2,...]. Please provide me with 20 prompts.".

12 LIMITATIONS

We introduce three types of reward models, CLIP Score (Hessel et al., 2021), ImageReward (Xu et al., 2023), and VQAScore (Lin et al., 2024) in the training process. However, these reward models are usually used to enhance text-image alignment or align with human feedback. Training a reward model of higher quality is of great significance for enhancing the reasoning ability of image generation models. We will reserve this for future work. Introducing better reward models can improve the accuracy of the reward function, leading to the broader application of reinforcement learning in image generation.

13 THE USE OF LARGE LANGUAGE MODELS (LLMS)

We use the LLM to polish the manuscript in order to enhance its readability. This includes correcting word choice and grammatical errors in the paper to achieve more polished writing.